J Mater Sci (2008) 43:892–899
DOI 10.1007/s10853-007-2181-x

Special WC/Co orientation relationships at basal facets of WC grains in WC–Co alloys

Valérie Bounhoure · Sabine Lay · Marc Loubradou · Jean-Michel Missiaen

Received: 20 July 2007 / Accepted: 21 September 2007 / Published online: 31 October 2007

Abstract In WC–Co alloys prepared by liquid phase sintering WC grains are partly surrounded by the Co binder and are terminated by basal and prismatic facets. This work reports transmission electron microscopy (TEM) observations on basal WC/Co interfaces. Two kinds of preferred orientation relationships are found. The one most common corresponds to the joining of $(0001)_{WC}$ with $(111)_{Co}$ planes. It leads to a large parametric misfit of 15% and is observed for only small pools of Co, mainly located in corners formed by the contact between WC grains. The second type of interface corresponds to the joining of $(0001)_{WC}$ with $(001)_{Co}$ and is more rarely found. For random WC/Co orientation relationships a thin WC_{1-x} cubic layer about two atomic rows is revealed at the interface.

Introduction

WC–Co hard materials are obtained by the powder metallurgy route, usually after liquid phase sintering. These alloys combine a high toughness with a high hardness making them suitable for a wide range of applications including tools and wear parts. After liquid phase sintering, WC grains are faceted [1]. They are delimited by basal and prismatic planes and are partly surrounded by the Co binder. This latter forms a skeleton inside the alloy. After cooling, large Co grains several μm in size are observed in agreement with [2]. This feature shows that the liquid is interconnected over large areas and that during cooling liquid Co crystallizes from a small number of nucleus. In this way, it is expected that no preferred orientation of Co regarding WC would occur except maybe for the nucleus that has solidified first. Up to now, little experimental work was devoted to the structure of WC/Co interfaces in the literature. Main results concern the affinity of the $(111)_{Co}$ habit plane with the $(0001)_{WC}$ plane reported from the observation of small Co inclusions in WC grain [3]. In other respects the existence of a thin ordered precursor film of Co on the basal surface of WC was suggested from wetting experiments at the solid state [4]. The effect of the C/W ratio should also be studied since it is known to influence the interface energetic of the system [5–7]. The aim of the present work is to get a better knowledge on WC/Co basal interfaces in WC–Co alloys after solidification. Special orientations of Co regarding $(0001)_{WC}$ are detected by transmission electron microscopy (TEM). Two kinds of interfaces are studied by high resolution TEM (HRTEM). A special feature of random WC/Co interfaces is revealed using HRTEM.

Materials: preparation and data

Several types of WC–Co alloys were examined (Table 1). The effect of the C/W ratio is studied owing to the C and W rich alloys called WC–Co,C and WC–Co,W. The C or W addition leads to the presence of graphite or $(Co,W)_6C$ in the mixture of WC and Co. The other alloys contain some Cr and are called WC–Co,Cr or WC–Co,C,Cr depending on the C rate. The Co for Cr substitution rate (5%) is close to that in industrial grades. The alloys were prepared from WC powder with 0.91 μm in size and were heated at 1200°C for 1 h under argon flow then heated up to 1450°C

V. Bounhoure · S. Lay (✉) · M. Loubradou · J.-M. Missiaen
Science et Ingénierie des Matériaux et Procédés,
INPGrenoble-CNRS-UJF, BP75, St Martin-d'Hères
Cedex 38402, France
e-mail: sabine.lay@ltpcm.inpg.fr

Table 1 Measured contents of the alloys (at.%) after the sintering treatment

	W	C	Cr	Co
WC–Co,C	42.55	44.45	–	13
WC–Co,W	44.4	42.8	–	12.8
WC–Co,Cr	43.8	43.5	0.6	12.1
WC–Co,C,Cr	42.4	44.55	0.65	12.4

then maintained at 1450°C for 2 h using the processing conditions described in detail in [8]. The cooling time, is about 10 min in the temperature interval 1450–600°C.

Thin slices 30 μm thick were prepared by mechanical thinning for TEM observations. They were then milled by argon ions at an angle of 10°. TEM observations were performed using a 200CX JEOL or a 3010 JEOL microscope. The HRTEM study was carried out using a 4000EX JEOL microscope operated at 400 kV (C_s = 1.05 mm, semi-convergence angle 0.8 mrad, focus spread 9 nm). The contrast of the HRTEM images was simulated using the EMS software [9]. The interfacial dislocations were studied using the HRPACK software that calculates the displacement field around crystal defects [10].

Electron diffraction experiments and HRTEM images were interpreted using the lattice parameters of the system [11]. WC has a hexagonal unit cell (P-6m2) with W atoms at (0,0,0) and C atoms at γ (1/3,2/3,1/2) or β (2/3,1/3,1/2) positions. Its lattice parameters are a = 0.2906 nm and c = 0.2837 nm. In WC–Co alloys, Co is a face centered cubic metal with space group Fm-3m and Co atoms in (0,0,0) position. Some W and C atoms are dissolved in the binder and modify its lattice parameter [12]. As a first approximation the lattice parameter of pure Co equal to 0.3544 nm is used.

Results

(0001)WC//(111)Co interfaces

Transmission electron microscopy observations of the Co binder detect small Co pools with an orientation different from that of the Co matrix mainly located in corners formed by the contact between WC grains (Fig. 1). Diffraction experiments show that these small Co pools are oriented preferentially regarding basal facets of neighboring WC grains. In some cases the orientation relationship could be determined as follows [13]:

$$(0001)_{WC}//(111)_{Co} \quad \text{with} \quad [2-1-10]_{WC}//[-110]_{Co}$$

This orientation will be called OR1. The orientation OR1 was observed in all studied alloys. It is noticeable that it corresponds to the relationship reported by [3] for Co inclusions in WC grains. The lattices of WC and Co do not match well for this orientation. A parametric misfit of about 15% can be calculated and is illustrated in Fig. 2. This misfit is very large compared to the values close to 2% usually observed for interfaces.

The HRTEM technique was used to study this interface and find out how such a large misfit could be compensated. Figure 3 shows a HRTEM image of a WC/Co interface oriented according OR1 in the WC–Co,C alloy. A dense dislocation network is observed at the interface. The mean dislocation spacing is close to 1.5 nm what corresponds to $7d_{(-1-12)Co}$ or to $6d_{(01-10)WC}$ where $d_{(-1-12)Co}$ and $d_{(10-10)WC}$ are the spacing between (–1–12) planes in Co and (01–10) planes in WC. The interface structure was determined in several steps. The HRTEM image contrast was first interpreted using image simulation. Then the structural unit at the interface was determined from the atom positions between two dislocations. Finally, the elastic field around the dislocations was simulated and compared to the experimental image.

Several HRTEM images with increasing defocus values were recorded for this interface. The focus values f were determined by analyzing the image contrast of the amorphous layer at the edge of the hole close to the interface [14]. For Fig. 3 a value close to –30 nm was deduced. Some disordering of the atom columns was observed close to the hole so a suitable distance in between 10 and 20 nm from the edge of specimen was chosen to study the interface. The thickness of the studied areas could be estimated to be in the range 3.5–7 nm. The contrast of Co and WC was simulated for focus values close to –30 nm and specimen thicknesses up to 10 nm. It was observed that the specimen thickness has only a little influence on the features of the images. A value of 6 nm was taken. The qualitative comparison of the experimental and simulated images shows a good fit at f = –25 nm for both WC and Co lattices (Fig. 4). This value is in the uncertainty range of the focus determination and will be used in what follows.

Comparing the contrast of the calculated images and the atom positions shows that Co and W atomic columns lie in dark areas at the centers of polygons formed by the white dots (Fig. 4g). C atomic columns lie in an outer part of the white dots. The positions of Co and W atomic columns can therefore be deduced from the experimental image unlike those of C atomic columns. The atom stacking across the interface was then determined from the experimental image using small parts of the interface between two dislocations to decrease the effects of distortions close to the dislocation cores. It was determined as ACBAAA (Fig. 5a).

This stacking was checked by introducing the atom shifts around the dislocations. Their Burgers vector could be first determined using a Burgers circuit [15]. No step is

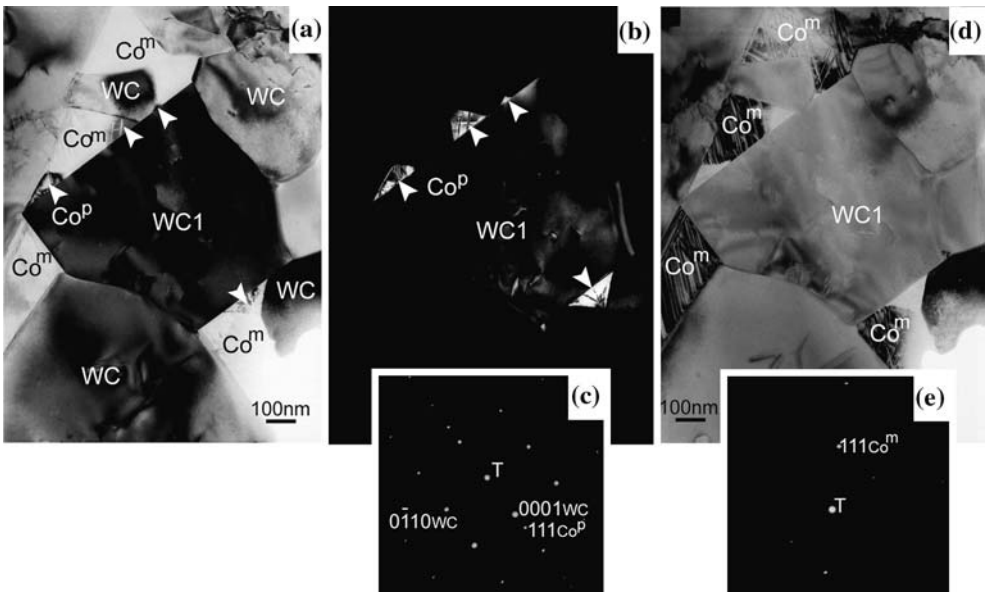

Fig. 1 Examples of misoriented Co pools observed in the WC–Co,Cr alloy. (**a**) Bright field TEM image showing WC grains in contact with the Co matrix called Co^m. In the matrix, some small Co pools with a darker contrast denoted Co^p are arrowed. (**b–c**) Dark field image obtained with $g = 111Co^p$ and associated diffraction pattern of a region containing WC1 and a small pool. The diffraction pattern shows the preferred orientation of Co^p regarding (0001) plane of WC1. (**d–e**) Bright field image of the same area obtained for another orientation and associated diffraction pattern of the Co matrix. The (111) reflection of Co^m is close to the Bragg position, which leads to a dark contrast of the Co matrix unlike the Co pools that have another orientation

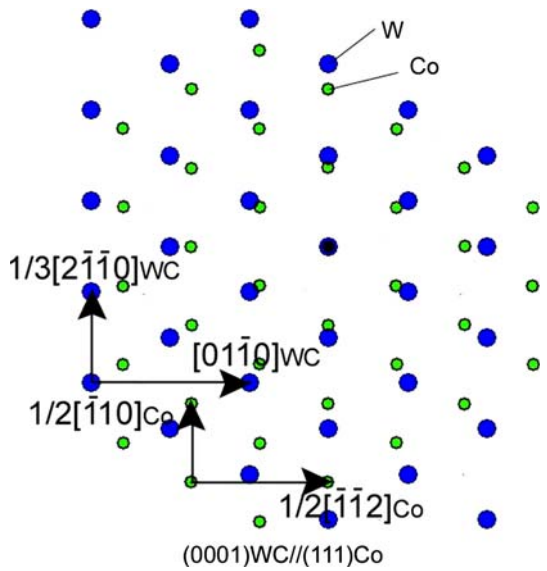

Fig. 2 Superposition of the (0001)WC and (111)Co planes oriented according to OR1 showing the large misfit between atomic positions of both lattices. For WC, a W atoms containing plane was chosen. The spacing value between two W atoms is 0.2906 nm and the spacing between two Co atoms is equal to 0.252 nm in these planes what leads to a parametric misfit of 15%

associated with the dislocations. The projected component of the Burgers vector is the same for all dislocations. It is parallel to the interface plane and is equal to $\frac{1}{4}[-1-12]_{Co}$. It compensates for the parametric misfit between $(-1-12)_{Co}$ and $(01-10)_{WC}$ spacings. A screw component equal to $\pm\frac{1}{4}[-110]$ must be added to relate the nodes of WC and Co lattices. The total Burgers vector of the dislocations is therefore equal to $b_1 = \frac{1}{2}$ [–101] or $b_2 = \frac{1}{2}[0-11]$.

The displacement field of the dislocations was introduced in the calculated positions of atom columns across the interface using the HRPACK program (Fig. 5a). It is seen in Fig. 5b that they fit well with the experimental image and validates the sequence ACBAAA. The position of the interface can be determined by a careful inspection of the HRTEM image (Fig. 5b). The interplanar distance between planes in Co parallel to the interface is the one of $(111)_{Co}$ planes (= 0.205 nm). The distance between planes in WC is the one of $(0001)_{WC}$ planes (= 0.284 nm). At the interface, the distance between planes is an intermediate value (= 0.24 nm). The atomic stacking from Co to WC can therefore be written as ACBA/AAA. According to this sequence, four kinds of models can be assumed by introducing C atoms in the WC lattice in position γ or β (Fig. 6):

ACBA/γAγAγA	I
ACBA/βAβAβA	II
ACBA/AγAγA	III
ACBA/AβAβA	IV

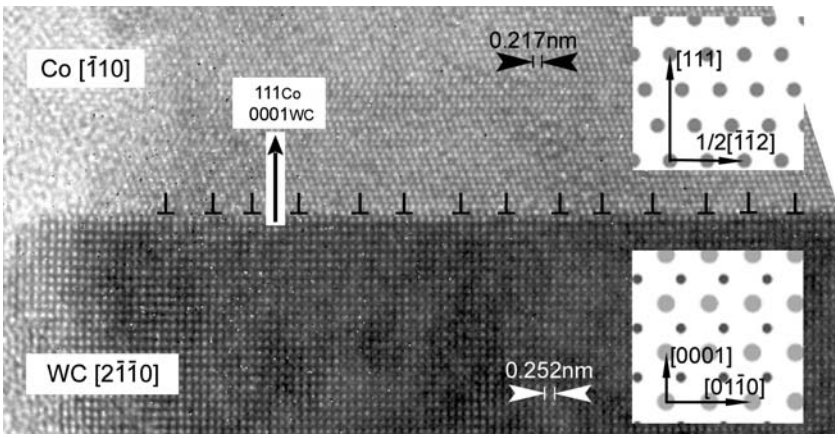

Fig. 3 HRTEM image of a WC/Co interface with the OR1 orientation observed in the WC–Co,C alloy

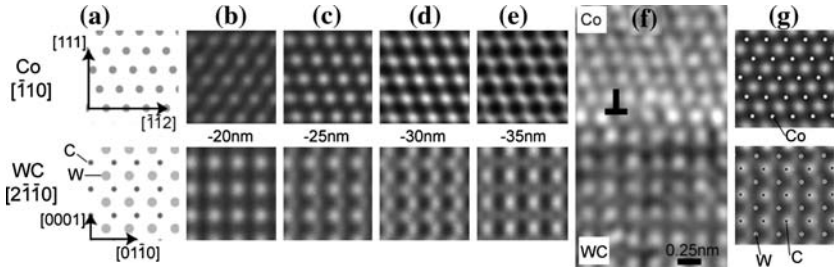

Fig. 4 (**a**) Projection of Co and WC crystal lattices along the studied directions. (**b**–**e**) Image simulations of the lattices for f equal to –20 nm up to –35 nm and a specimen thickness of 6 nm. (**f**) Magnification of the experimental HRTEM image shown in Fig. 3. The best fit occurs for $f = -25$ nm. (**g**) Superposition of the atom positions and of the images simulated for $f = -25$ nm

For sequences I and II the WC facet is C terminated while for sequences III and IV it is W terminated. The contrast of the models was simulated using atom boxes including the interface dislocations (Fig. 7). No significant difference in contrast compared to the experimental image can be found at the interface. Therefore no model can be eliminated.

These results can be discussed in the framework of a theoretical study on the stability of WC/Co interfaces with the orientation OR1 [7]. Using ab-initio calculations the energy of eight interfacial geometries was determined. The models correspond to different translations between the crystals. In this study only the translation parallel to the interface plane is described. The translation perpendicular to the interface plane is not mentioned. Moreover, only the first layer of Co atoms close to the interface is taken into account in the calculations. The comparison with our finding shows that sequences I and II correspond to the model called d while sequences III and IV correspond to models a or b in Fig. 1 of [7]. The C ended model d has a lower energy (1.16 J/m^2) than a (3.15 J/m^2) and b (1.45 J/m^2). It is to note that the experimentally found structure does not fit with the C ended model called c that has the lowest energy (0.66 J/m^2). From these data, it is expected that the

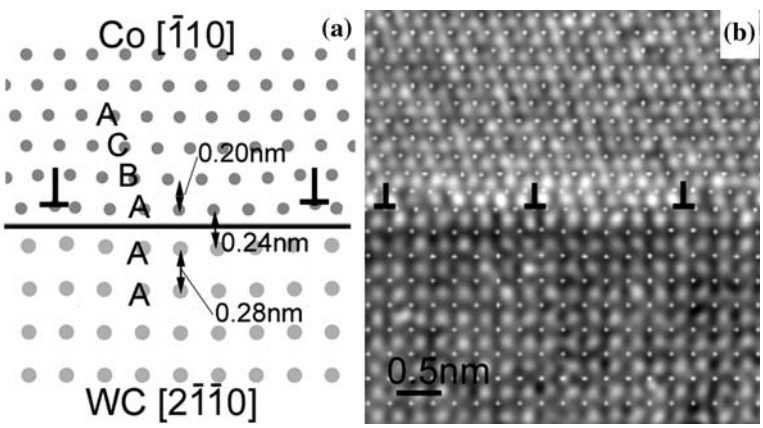

Fig. 5 (**a**) ACBAAA sequence at the interface and displacement field associated to the interface dislocations. (**b**) Superposition of the calculated atom positions on the experimental HRTEM image

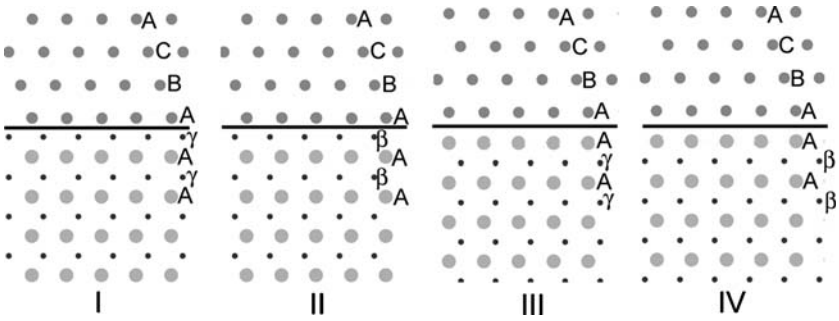

Fig. 6 Models corresponding to the atom sequence deduced from the experimental HRTEM image of Fig. 5

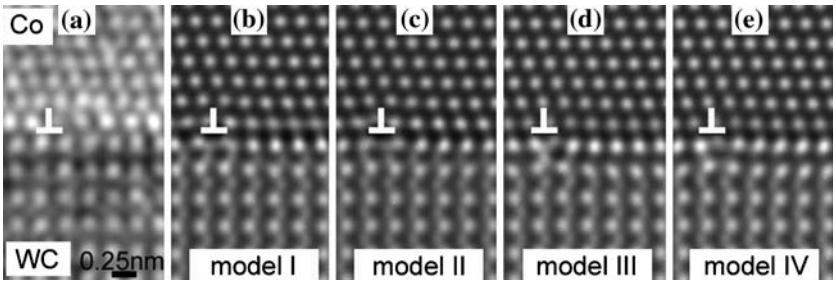

Fig. 7 (**a**) Experimental HRTEM image and (**b**, **e**) images simulated for models I–IV (f = –25 nm and thickness = 6 nm). For models I (III) and II (IV), the image of WC is slightly different, but this difference is not detected on the experimental image

sequences I or II are the best candidates for the studied interfacial structure.

The inspection of the superimposition of (0001)WC and (111)Co planes (Fig. 2) shows that a good fit of the crystals occurs if one lattice is rotated 30° around the normal of the interface plane regarding OR1 (Fig. 8). This orientation relationship is called OR2 and can be described as follows:

$$(0001)_{WC}//(111)_{Co} \quad \text{with} \quad [1-100]_{WC}//[-110]_{Co}$$

From the superimposed lattices a good matching of some atomic sites is observed: one node over three is in coincidence for the W lattice and one node over four for the Co lattice. Moreover, the misfit value for these coincident sites is very small and is equal to 0.4%. The main difference between the orientation relationships OR1 and OR2 is the density of sites in coincidence. For OR1, all sites are in coincidence if we except the misfit while only one site over three or four is in coincidence for OR2. Up to now, this kind of orientation was not evidenced experimentally although it is expected on the basis of the coincidence site lattice concept [16].

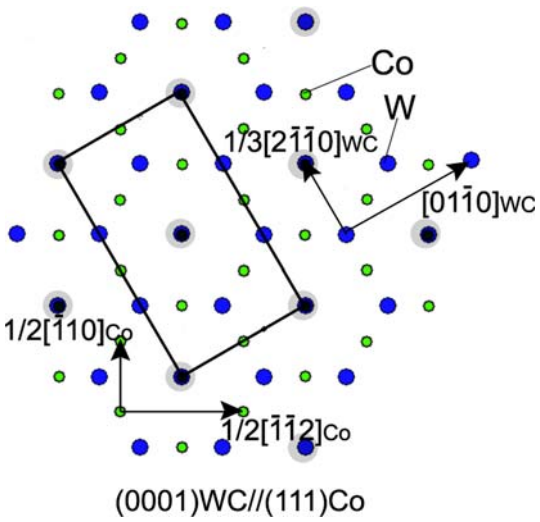

Fig. 8 Superposition of the (0001)WC and (111)Co planes according OR2 showing the planar coincidence cell for this orientation

(0001)WC//(001)Co interfaces

Another orientation relationship is pointed out using HRTEM in the WC,Co,CCr alloy sintered for 2 h at 1450°C. In Cr doped alloys the Cr enrichment of WC/Co interfaces was pointed out [17] and the presence of a thin MC carbide layer (M = W,Cr) forming on the surface of WC grains was shown [18]. For the studied interface, no MC layer is observed between WC and Co. A direct contact occurs between the $(001)_{Co}$ and $(0001)_{WC}$ planes (Fig. 9). The lack of the MC layer is related to the special orientation relationship called OR3 observed for this interface:

$$(0001)_{WC}//(001)_{Co} \quad \text{with} \quad [2-1-10]_{WC}//[110]_{Co}$$

In order to determine the degree of matching at the interface, the two planes $(0001)_{WC}$ and $(001)_{Co}$ are superimposed (Fig. 10). A near coincidence site lattice is found with a misfit value within the 0.4–3.2% interval and a

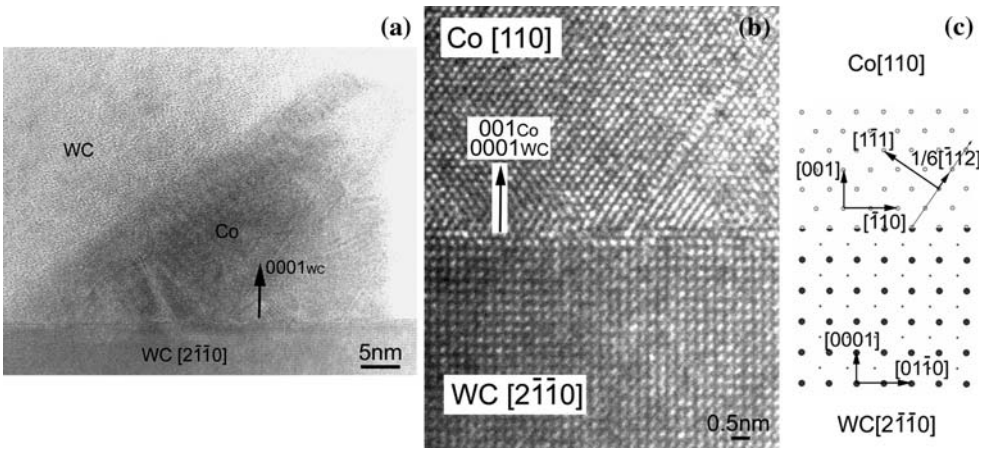

Fig. 9 (**a**) General image of a Co pool in special orientation relationship with the lower WC grain in the WC–Co,C,Cr alloy. (**b**) HRTEM image of the WC/Co interface. The orientation of Co is determined from the projection of the atoms. (**c**) Picturing the atom positions at the WC/Co interface

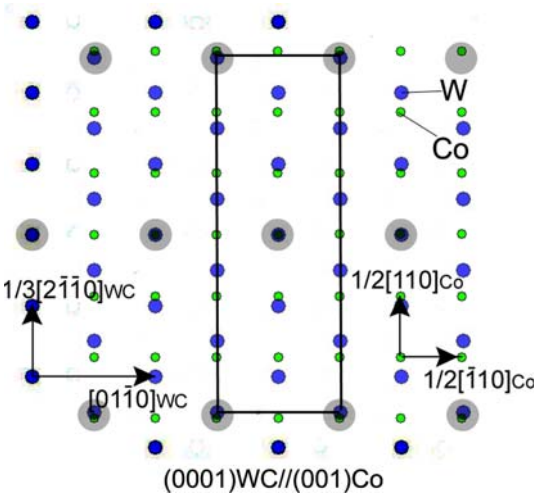

Fig. 10 Superimposition of the (0001)WC and (001)Co planes according to OR3 showing the planar coincidence cell for this orientation. A small misfit of 0.4% occurs in [–110] direction while a mismatch of 3.2% is recorded in the [110] direction

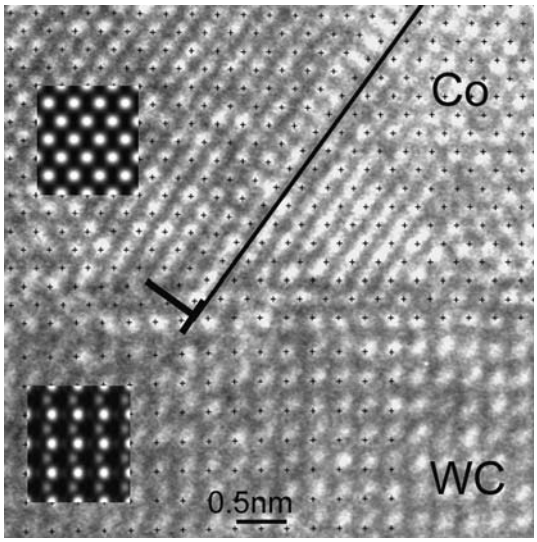

Fig. 11 Superimposition of the calculated positions of atom columns around the stacking fault on the HRTEM image. Two inserts are added showing the simulated contrast of WC and Co for f = –60 nm and a thickness of 6 nm. The partial dislocation lies at the interface

coincidence ratio rather large: one site over five is in coincidence for W sites and one over six for Co sites. This good matching probably explains the formation of such an interface. Along the direction [–110]Co //[01–10]WC, the misfit value is close to zero.

As expected few defects are noticed at the interface along this direction (Fig. 9b). Only several stacking faults lying in Co and stopping at the interface are observed. The focus value of the HRTEM image was evaluated close to –60 nm owing to the experimental conditions used and the contrast analysis of the amorphous layer. The image quality is less good than in the previous case so no attempt will be made to determine the nature of the atoms at the interface. Image simulation shows that the white dots of the image correspond to Co and W columns for focus values close to –60 nm. The Burgers vector of the partial dislocations attached to the fault and lying in the interface was determined as bp = 1/6[–112] from the geometry of the defect and using the HRPACK program (Fig. 11). Since the binder contains W, C, and Cr atoms, its parameter slightly deviates from the one of Co. It is therefore difficult to predict the exact value of the parametric misfit at the interface. The component of bp parallel to the interface is oriented in such a manner that the dislocation can compensate for a spacing of $(–110)_{Co}$ planes smaller than the one of $(01–10)_{WC}$ planes at the interface.

Thin interfacial cubic layer

Special attention was devoted to random WC/Co interfaces in order to detect a local interfacial ordering. Actually HRTEM observations point out the presence of a thin film about two atomic rows at the interfaces with a high

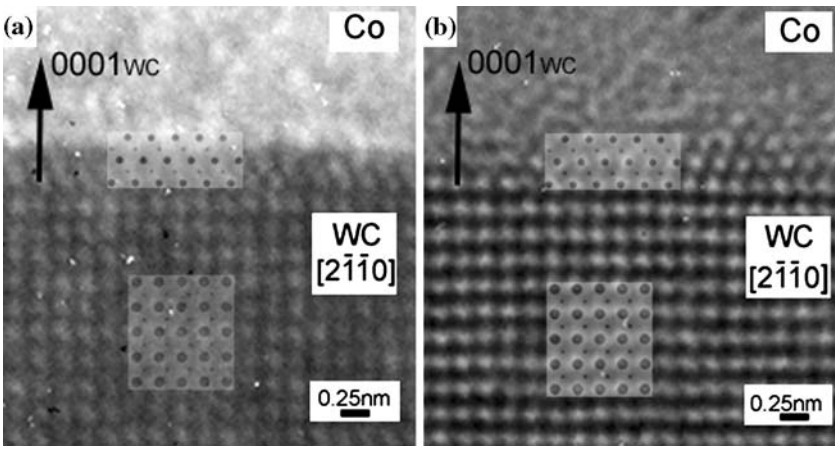

Fig. 12 HRTEM images of WC/Co random interfaces in (**a**) WC–Co,C and (**b**) WC–Co, W sintered for 2 h at 1450°C. A thin cubic layer is visible at the interface. A good fit with WC_{1-x} lattice is found for the interface film

frequency in WC–Co,W and more seldom in WC–Co,C (Fig. 12). The atomic stacking in the layer corresponds to a cubic crystal oriented along [1–10] with (111) plane parallel to $(0001)_{WC}$. Two crystal lattices can be assumed for this compound. Co is candidate in the assumption of a thin layer with an orientation different from the Co binder above the interface. The cubic WC_{1-x} compound that is stable at higher temperature is also considered owing to the elements present in the alloys [19]. Indeed, thin $(M,W)C_{1-x}$ cubic layers with M being Cr or V were already observed at WC/Co interfaces in doped alloys [18, 20]. The lattices of Co and WC_{1-x} were carefully superimposed on the HRTEM images. Due to the smaller lattice parameter of Co compared to WC_{1-x} ($a = 0.4336$ nm [11]) the best fit occurs for WC_{1-x}. The parametric mismatch at the WC/WC_{1-x} interface is close to 5%. In order to get a better insight on the formation of this layer, the thickness of the layer was compared to the thickness of WC that precipitates on the surface of WC grains during cooling. The calculation was performed by considering the volume fractions of WC at 1450°C and 1000°C and making the excess of WC precipitate onto the existing grains. A mean shape and size of WC grains was assumed [8]. This calculation leads to a thickness larger than the one observed for the film, about 13 nm for WC–Co,C and 9 nm for WC–Co,W. The WC_{1-x} layer would then correspond to the last atomic layers which have precipitated during cooling.

Discussion and conclusion

The solidification of the binder phase in WC–Co alloys generally forms large Co crystals without preferred orientation with the embedded WC grains. However this study reveals the presence of local interfacial configurations which may minimize the interfacial energy.

First thin WC_{1-x} films are observed at random basal WC/Co. These films form at the end of the precipitation of W and C atoms at the surface of WC grains. The WC_{1-x} cubic carbide is C deficient so it can accommodate some deviation of stoichiometry especially in the W rich alloy where the film is observed very frequently. Its formation would be promoted by the C deficiency and by the lower interface energy of the WC/WC_{1-x}/Co sandwich compared to that of the WC/Co interface for random orientations. The thickness of the WC_{1-x} layer would be limited by the poor stability of this compound at low temperature and by the rather large parametric misfit with WC.

Second numerous small Co pools with an orientation different from that of the binder skeleton are present in all studied alloys. They are in contact with the basal facets of neighboring WC grains. These observations show that Co present in quasi-isolated liquid pools may crystallize independently of the surrounding matrix by forming nucleus which minimize the interface energy. The Co solid pools adopt two kinds of preferred orientation relationships. The one most commonly found corresponds to the joining with the (111) plane of Co, which leads to a misfit value of 15% and a coincidence ratio of 1. This rather large misfit is made possible by (i) the relaxation of stresses by the formation of a dense interfacial dislocation network and (ii) the coincidence between dense planes of both WC and Co structures, which maximizes the chemical bounding at the interface. The other orientation is due to the joining with the (001) plane of Co. A smaller misfit value is recorded (0.4–3.2%) while the coincidence ratio is smaller ($< 1/4$). A third special orientation is expected from the coincidence site lattice concept but is not found in this work. A systematic study using the electron backscatter diffraction technique in a scanning electron microscope would provide more quantitative information on this point.

Acknowledgements We thank Sandvik Hard Materials for financial support and P. Bayle of CEA Grenoble for availability of the 4000EX microscope. We also thank Pr. G. Wahnström for fruitful discussion on WC/Co interface energetics.

References

1. Exner HE (1979) Int Metal Rev 24:149
2. Sarin VK, Johannesson T (1975) Metal Sci 9:472
3. Mohan K, Strutt PR (1996) Mat Sci Eng A 209:237
4. Göthelid M, Haglund S, Ågren J (2000) Acta Mater 48:4357
5. Kim S, Han SH, Park JK, Kim HE (2003) Scripta Mater 48:635
6. Schubert WD, Bock A, Lux B (1995) Int J Refract Metal Hard Mater 13:281
7. Christensen M, Wahnström G, Lay S, Allibert CH (2007) Acta Mater 55:1515
8. Wang Y, Heusch M, Lay S, Allibert CH (2002) Phys Stat Sol A 193:271
9. Stadelmann P (1987) Ultramicroscopy 21:131
10. Bonnet R, Loubradou M (1997) Ultramicroscopy 69:241
11. Villars P, Calvert LD (1985) Pearson's handbook of crystallographic data for intermetallic phases. vol. 2. American Society for Metals, Metals Park
12. Maritzen W, Ettmayer P, Kny E (1985) Powder Metall Int 17(2):68
13. Lay S (2006) In: Proceedings of the Euro PM2006 Congress and Exhibition, Gand, October 2006, The European Powder Metallurgy Association, vol. 1 Hard Materials, p 55
14. Spence JCH (1988) Experimental high resolution electron microscopy. Oxford University Press, New York
15. Hirth JP, Lothe J (1968) Theory of dislocations. McGraw-Hill Book Company, New York, McGraw-Hill Series in Materials Science and Engineering
16. Bollmann W (1970) Crystal defects and crystalline interfaces. Springer-Verlag, Berlin
17. Yamamoto T, Ikuhara T, Watanabe T, Sakuma T, Taniuchi Y, Okada K, Tanase T (2001) J Mater Sci 36:3885. doi:10.1023/A:1017953701641
18. Delanoë A, Bacia M, Pauty E, Lay S, Allibert CH (2004) J Cryst Growth 270:219
19. Nagender Naidu SV, Sriramamurthy AM, Rama Rao P (1991) In: Nagender Naidu SV, Rama Rao P (eds) Phase diagrams of binary tungsten alloys, monograph series on alloy phase diagrams. The Indian Institute of Metals, Calcutta, p 37
20. Lay S, Hamar-Thibault S, Lackner A (2002) Int J Refract Metal Hard Mater 20:61